IEEE Access
Multidisciplinary ⋮ Rapid Review ⋮ Open Access Journal

Received 25 May 2025, accepted 28 June 2025, date of publication 4 July 2025, date of current version 22 July 2025.

Digital Object Identifier 10.1109/ACCESS.2025.3586112

RESEARCH ARTICLE

Numerical Study on Human Brain Cortical Electrostimulation Assessment During Uniform Magnetic Field Exposure at Intermediate Frequencies

JOSE GOMEZ-TAMES[1,2], (Member, IEEE), THOMAS TARNAUD[3,4], WOUT JOSEPH[3], (Senior Member, IEEE), AND EMMERIC TANGHE[3]

[1]Graduate School of Science and Engineering, Chiba University, Chiba 263-8522, Japan
[2]Center for Frontier Medical Engineering, Chiba University, Chiba 263-8522, Japan
[3]Department of Information Technology (INTEC), Ghent University-imec, 9052 Ghent, Belgium
[4]Department of Head and Skin, Ghent University, 9000 Ghent, Belgium

Corresponding author: Jose Gomez-Tames (jgomez@chiba-u.jp)

The work of Jose Gomez-Tames was supported by the Japan Society for the Promotion of Science (JSPS) Grant-in-Aid for Scientific Research, JSPS KAKENHI, under Grant 23K25176 and Grant 25K15887. The work of Thomas Tarnaud was supported by FWO-V (Research Foundation Flanders) under Grant 1230222N.

ABSTRACT Permissible limits have been established by international guidelines and standards for human protection against electromagnetic field exposure to prevent adverse health effects stemming from electrostimulation in the most sensitive body part. That is the peripheral nervous system (PNS) in the intermediate frequency range (300 Hz to 100 kHz) and the central nervous system (CNS) at lower frequencies. However, there is a need to reevaluate protection limits against CNS electrostimulation in the intermediate frequency range, considering the importance of brain tissues during electromagnetic head exposure. This study aims to derive the level of CNS cortical stimulation to evaluate compliance with existing protection limits. To achieve this, a numerical multi-scale model was used to evaluate neuron stimulation thresholds by integrating individual neurons into realistic anatomical head models. Five different excitable membrane models within the motor cortex were examined across three human head models, providing the most comprehensive and extensive evaluation to date. The results show that current protection limits are confirmed as conservative, with non-compliance observed in only 0.02% and 2.4% of axons under clamped and sealed boundary conditions, respectively. The study also highlights significant intersubject variability (up to a 600% mean threshold) and clarifies the influence of neural excitation models on permissible level assessments. In conclusion, current electric field limits are conservative for CNS electrostimulation in the intermediate frequency range, but the margin of safety decreases at higher frequencies, warranting further evaluation. The study's findings and methodology contribute to the rationale and provide valuable insights for re-evaluating electromagnetic safety exposure guidelines.

INDEX TERMS Dosimetry, electric field, intermediate frequency, multi-scale modeling, nerve model, protection limits.

I. INTRODUCTION

International guidelines (ICNIRP [1] and IEEE ICES [2]) aim to prevent adverse health effects from non-ionizing electromagnetic field exposure by setting [1], [2] exposure limits based on electrostimulation and thermal effects. Electrostimulation effects dominate at lower frequencies (up to 100 kHz for continuous exposure and up to 5–10 MHz for brief pulse exposures). At higher frequencies, thermal effects from energy absorption become the primary concern. Both guidelines apply safety margins, distinguishing between public (unrestricted) and occupational (restricted) exposure scenarios.

The associate editor coordinating the review of this manuscript and approving it for publication was Wei Xu.

Limits are defined for the most sensitive region. For the intermediate frequency range (∼400 Hz in ICNIRP and ∼750 Hz to 100 kHz in IEEE), the peripheral nervous system (PNS) has been adopted as the basis for limits. In the IEEE standard, the PNS threshold is derived from the electric field threshold required to stimulate a 20 μm straight axon fiber model (SENN: spatially extended nonlinear node) in a uniform isotropic medium, using Frankenhaeuser-Huxley (FH) membrane dynamics [3], which is consistent with experimental thresholds [4]. Central nervous system (CNS) thresholds are derived using the same nerve modeling criteria as for the PNS (except that the PNS and CNS axon model diameters are 20 μm and 10 μm, respectively). CNS safety limits also consider adverse synaptic effects based on phosphenes thresholds as a surrogate. In this frequency range, PNS shows lower activation thresholds than CNS.

However, the assumption of considering the same neural model for CNS and PNS raises concerns. First, excitation thresholds vary significantly across different membrane dynamics models [5]. The SENN model relies solely on FH dynamics, which may not adequately represent CNS neuron behavior.

Second, neural axons with diameters up to 20 μm have been reported in CNS structures [6]. Including these larger fibers would result in lower (less conservative) stimulation thresholds. Third, the assumption of a uniform, isotropic, and homogeneous medium oversimplifies the complex anatomical geometry [7]. High conductivity contrasts in the head, at interfaces such as cerebrospinal fluid (CSF) and gray matter, can create local electric field hotspots and significant spatial gradients. These effects can influence stimulation beyond the axon terminal mechanism assumed in PNS models [8]. Finally, individual anatomical differences and complex nerve trajectories within convoluted gray matter regions are not accounted for in current standards, which assume straight axon models [1], [2]. Axonal bends, in particular, are known to be sites of reduced activation thresholds and should be considered [3].

These factors highlight the need for more comprehensive modeling specific to CNS tissue when deriving exposure limits for electromagnetic safety at intermediate frequencies [8]. In this context, multi-scale simulations that couple electric field analysis in biological tissues (millimeter scale) with neuron models (micrometer scale) are necessary [9], as outlined in the research agenda of IEEE ICES [10]. Likewise, ICNIRP recommends conducting excitation modeling and threshold assessments to refine permissible exposure levels [11]. Therefore, there is a need to estimate neuronal activation thresholds under more realistic scenarios [9], [12], [13], particularly given the limited experimental data available in the intermediate frequency range [14].

A working group within the IEEE ICES Technical Committee 95 Subcommittee 6, led by the authors, was established to explore electrostimulation thresholds in the brain. Initial efforts evaluated the consistency of the multi-scale computations and assessed the conservativeness of permissible field strengths in international guidelines at intermediate frequencies [15]. However, a comprehensive assessment of CNS stimulation in this frequency range remains lacking.

This study aims to investigate brain cortical stimulation thresholds, considering various classical neural models and individual differences in head anatomy, using a multi-scale computational approach for uniform magnetic field exposure at intermediate frequencies (300 Hz to 100 kHz). Moreover, the conservativeness of protection limits in international guidelines is investigated. Importantly, the results and methodology of this study could contribute to the rationale and refinement of international safety standards by providing a more accurate scientific basis for protection and serving as input for the re-evaluation of the guidelines and the conservativeness of the limits in the intermediate frequency exposure guidelines.

II. MODELS AND METHODS

A. HUMAN HEAD MODEL

Three realistic head models (all male, 41 years old, healthy) were created from freely available magnetic resonance imaging (MRI) data. The head models were voxelized with a resolution of 0.5 mm and consisted of 12 tissues/body fluids, as shown in [16].

B. ELECTROMAGNETIC COMPUTATIONAL MODEL

In the context of electrostimulation, the allowable quantity is estimated from the internal electric field induced within the exposed individual's body. At intermediate frequencies, the magneto-quasistatic approximation applies to the computation of the internal electric field in biological tissues. The electric and external magnetic fields are decoupled and treating the exposure to these fields separately is possible. Also, permittivity can be neglected; only tissue conductivity is considered, as the displacement currents are more than one order of magnitude smaller than the conduction currents [17]. Thus, the induced scalar electric potential ϕ is given by the following equation:

$$\nabla \cdot \sigma \nabla \phi = -\nabla \cdot \sigma \frac{\partial \boldsymbol{A}}{\partial t}, \tag{1}$$

where A and σ denote the magnetic vector potential of the applied (external) magnetic field and tissue conductivity, respectively. When (1) is solved, the internal electric field $\boldsymbol{E}$ is calculated: $\boldsymbol{E} = -. \nabla\phi - \mathrm{j}\omega\boldsymbol{A}_0$.

Equation (1) was solved numerically by the scalar potential finite difference method [18]. Tissue conductivities were assumed linear and isotropic and were determined using the fourth-order Cole-Cole model [19] at the frequencies corresponding to different exposure scenarios.

C. NEURONAL COMPARTMENT COMPUTATIONAL MODEL

We calculated stimulation thresholds of thick pyramidal axons extending from the hand motor cortex (Fig. 1A). Stimulation thresholds are identified when the induced electric field elicits action potentials in the cortical axon models.

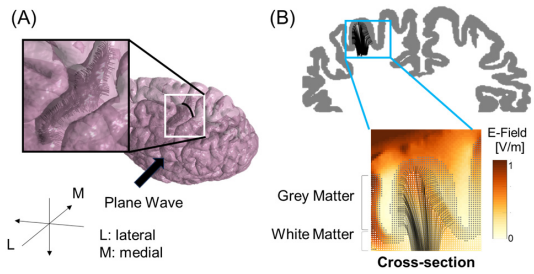

FIGURE 1. (A) Cortical axons are placed on the hand motor area (hand knob). (B) Cross-section plane showing the distribution of the axons and local electric fields induced by uniform exposure. The arrow is the direction of the uniform B-field.

The axon model from [3] is utilized, representing myelinated axons comprising internodes (segments covered by myelin sheaths) interspersed with nodes of Ranvier (short segments with a high ionic channel density) [20]. At the nodes of Ranvier, the ionic membrane current is formulated based on five classical models that follow a conductance-based voltage-gated model. These classical membrane models were the five earliest Hodgkin-Huxley type models obtained from patch clamp data. They were chosen for this study, because they are used frequently in computational neuroscience or neural engineering studies [21], e.g., for modelling of the human cochlear nerve and conduction block [[21], [22]]). In particular, the Frankenhaeuser-Huxley model (FH) has been used in the IEEE ICES C95.6 and C95.1 standards [2] and in the ICNIRP 2010 guideline [10] To make the Hodgkin-Huxley (HH) model compatible with the myelinated axon model, the nodal conductivity and capacitance values were scaled, as in [23]. At the internodes, the membrane current was modelled by the passive conductance multiplied by the membrane potential.

Neural activation is driven by the extracellular potential along the axons (Fig. 1B). The extracellular potential is estimated as a local linear integral of the internal electric field along the axon trajectory (resulting in a ''quasipotential'', because the electric field is not conservative in general. The elicitation of an action potential is considered when the membrane potential is depolarized and exceeds 50 mV, with either propagation over at least four consecutive nodes of Ranvier in either direction, or symmetrical propagation in both the ortho- and antidromic directions over two nodes of Ranvier [5]. Thus, the threshold can be expressed as the required internal electric field (or external magnetic field strength) to elicit an action potential.

Two boundary conditions were selected to approximate a terminating axon without considering other parts of the neuron (soma, axon collaterals, and dendritic tree). The sealed boundary condition is normally used as boundary conditions at the terminations of axon collaterals (e.g., [24]). The voltage clamp boundary condition considers that the axon end does not exist by assuming a fixed value equal to the resting potential of the node of Ranvier. This boundary condition is motivated by the observation that, in reality, there would be a connection with the soma instead of this termination. Here, voltage clamp conditions might be a good first approximation for the axial current running from the axon terminal towards the soma.

D. EXPOSURE SCENARIOS

We explored the influence of uniform exposure (300 Hz, 1 kHz, 10 kHz, 100 kHz) on neural activation of cortical axons (using 5 membrane models) embedded in three head models. We direct a uniform magnetic field (vector potential A in (1) is defined such that the magnetic field is constant) from the lateral to medial direction with continuous sinusoidal pulses (Figure 1A). We opted for this direction due to its lower thresholds for the axons projecting from the putative hand motor area compared to the two other conventional uniform magnetic field exposure directions (anterior-posterior and superior-inferior) [15].

Fast-conducting thickly myelinated pyramidal tract axons (Betz cell's axon) were considered for the hand motor area (20 μm in diameter [6]). An average of approximately ten thousand neural axons are projected from the hand motor cortex of each head model [25], as illustrated in Figure 1B. These axons traverse the gray-white matter boundary nearly perpendicular, ultimately forming the pyramidal tracts. Considering the influence of the electric field on axon bending, we integrated the bending of pyramidal cell axons into our model for axonal projection from the gyral wall and crown. These axon pathways were situated within the putative hand knob region of the primary motor cortex, approximately 2.5 mm beneath the cortical surface. A detailed explanation of how we generated pyramidal axon models can be found in [25].

E. DATA ANALYSIS

Post-processing techniques are implemented to effectively mitigate outliers in electric field values inherent when using voxelized anatomical models, where curved boundaries are approximated with a stair-step method. The 99th percentile field strength in the brain cortex is used to mitigate computational artifacts in the standards for scenarios of uniform exposure [26]. For a specific tissue, the 99th percentile value of the electric field is the relevant value to be compared with internal allowable quantities. This quantity is termed dosimetric reference limit (DRL) in IEEE and basic restriction (BR) in ICNIRP. ICNIRP delineates its restrictions based on two categories: one applicable to the general public and another to occupational exposure, where the latter permits higher thresholds (less conservative). Meanwhile, IEEE classifies exposure scenarios as either restricted or unrestricted environments.

III. NUMERICAL RESULTS

A. ELECTRIC FIELD DISTRIBUTION AND NEURAL ACTIVATION

Figure 2 shows activation maps at frequencies from 300 Hz to 100 kHz depicting the electric field threshold for each axon projecting from the cortical surface of the hand knob. Internal electric field thresholds are observed to increase at higher

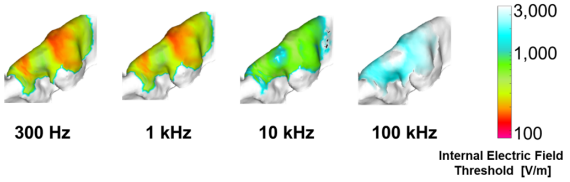

FIGURE 2. Spatial distribution of cortical activation thresholds at different frequencies on the hand motor area for one subject (7,358 cortical axons) for FH voltage clamped.

frequencies (a 35 and 8.3-fold increase over the range 300 Hz to 100 kHz of the mean and minimal thresholds, respectively). Also, despite some variability in the proportion of electrical conductivity among tissues at different frequencies, the shape of the activation maps remains consistent across the frequencies investigated. These observations were found to be consistent across all membrane neural models.

B. PERMISSIBLE FIELD STRENGTH

Figures 3 and 4 show that the stimulation thresholds increase with frequency, irrespective of the neuronal membrane and anatomical head models. In Figure 3, the stimulation thresholds of all axons show the conservativeness of all the protection limits in the clamped terminal condition, except for 0.3% of the CRRSS axons in subject 2 (S2) exhibiting thresholds below the limits at 100 kHz in the restricted environment (representing only 0.02% of all axons in the clamped condition at 100 kHz). Figure 4 shows that all axons comply with the limits for frequencies ranging from 300 Hz to 10 kHz for the sealed terminal. Also, all axons are compliant at 100 kHz, except for 4%-18% (CRRSS, S1-S3) and 5% (FH, S2) in the IEEE restricted environment (representing only 2.4% of all axons in the sealed condition). Figures 3 and 4 show that the most conservative limits are presented for lower-end frequencies (300 Hz −1 kHz). In the voltage-clamped terminal condition, there is a 22.5-fold gap between the minimum axon threshold and the unrestricted limit at 1 kHz (S2, HH model). The minimum gap is reduced to 5.2 and 2.3 times at 10 and 100 kHz, respectively. The gap is smaller in the sealed terminal condition to 10.9 times, 3.1 times, and 1.3 times at 300 Hz −1 kHz, 10 kHz, and 100 kHz, respectively. There is also an important difference between the membrane models. For lower-end frequencies (300 Hz −1 kHz), the FH and HH models present the minimum thresholds and are closer to the limits (sealed or clamped terminals). For the middle frequency (10 kHz), the HH, FH, and CRRSS models present smaller thresholds. For the end frequency (100 kHz), FH and CRRSS models present the minimum thresholds. The SE model shows the highest minimum thresholds for all frequencies. Threshold computation implemented in sealed end terminals reduces the threshold compared to clamped terminals by a factor of 6.7 to 106.

C. INDIVIDUAL DIFFERENCE

Figure 5 compares excitation thresholds among the three head models across all conditions. The ratios of mean and minimum thresholds were calculated with one head model serving as the common reference (e.g., S_3/S_1 and S_2/S_1). In voltage-clamped conditions (Figure 5A), the variations among mean ratio thresholds range from 0.2 to 1.7, while in sealed conditions (Figure 5B), they range from 0.7 to 2.6. This represents variations of up to 127% in the minimum threshold among the head models for a fixed membrane model, as well as boundary condition and frequency. The variation among average thresholds exceeds that among minimum thresholds, reaching up to 600%. We observed a larger intersubject variation of the mean threshold ratio in the voltage-clamped terminal than in the sealed terminal boundary condition across different frequencies and membrane models (a 3.6-fold increase in variation on average between both boundary conditions).

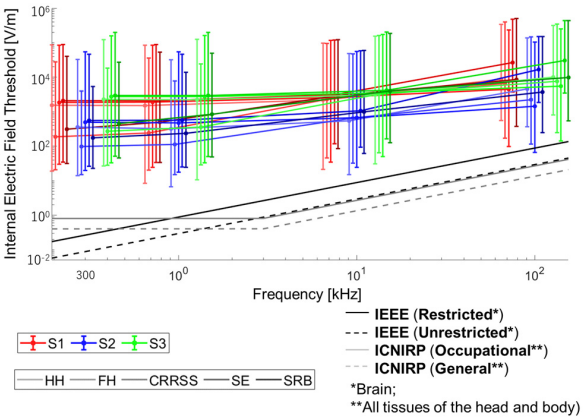

FIGURE 3. Excitation thresholds are estimated using the clamped terminal condition for uniform exposure compared with permissible internal limits of ICNIRP guidelines and IEEE safety standards. Excitation thresholds are plotted for 300 Hz, 1 kHz, 10 kHz, and 100 kHz: horizontal offsets between different subjects and membrane models are added for visualization. Abbreviations: HH: Hodgkin-Huxley, FH: Frankenhaeuser-Huxley, CRRSS: Chiu-Ritchie-Rogart-Stagg-Sweeney, SE: Schwarz-Eikhof, SRB: Schwarz-Reid-Bostock.

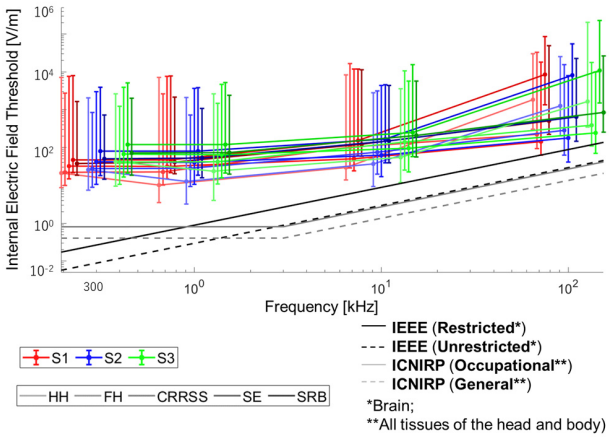

FIGURE 4. Excitation thresholds are estimated using a sealed terminal condition for uniform exposure compared with the permissible internal limits of ICNIRP guidelines and the IEEE safety standard. Excitation thresholds are plotted for 300 Hz, 1 kHz, 10 kHz, and 100 kHz: horizontal offsets between different subjects and membrane models are added for visualization. Abbreviations: HH: Hodgkin-Huxley, FH: Frankenhaeuser-Huxley, CRRSS: Chiu-Ritchie-Rogart-Stagg-Sweeney, SE: Schwarz-Eikhof, SRB: Schwarz-Reid-Bostock.

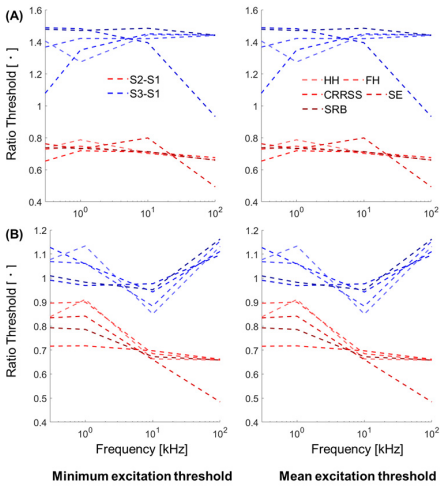

FIGURE 5. Ratio of threshold variations among three head models using one as common reference (S1) for (a) clamped and (b) sealed terminal conditions.

IV. DISCUSSION

This study examined CNS thresholds using axonal models projecting from the brain cortex to evaluate compliance with international electromagnetic exposure guidelines. IEEE Std C95.1-2019 specifies ERLs for whole-body exposure to prevent exceeding a DRL in the most sensitive regions. This corresponds to the PNS in the intermediate frequency. However, given the importance of CNS protection, it is necessary to revisit protection limits in this frequency range by incorporating axonal trajectories, anatomically realistic head models, and detailed membrane dynamics. Applying recent methodologies to investigate CNS thresholds will enhance the scientific basis of these standards and improve understanding of CNS exposure limits.

A. CONSERVATIVENESS

Conservativeness is investigated by considering various scenarios: five membrane models, an average of approximately ten thousand axonal fibers per head model, three head models, terminal conditions (sealed end or voltage clamped), and four frequencies (0.3, 1, 10, and 100 kHz). In total, we conducted more than 1.2 million exposure scenarios to evaluate the conservativeness of the limits. For the general public (unrestricted environment), conservativeness was confirmed for the ICNIRP and IEEE limits in all conditions. For occupational exposure (restricted environment), a marginal number of axons (0.02% among all voltage clamp boundary condition simulations) did not comply with the limits at 100 kHz. More non-compliant axons (2.4% among all conditions) were observed at the restricted environment levels at 100 kHz for sealed terminals.

B. TERMINAL BOUNDARY CONDITIONS

The selection of the terminal boundary conditions influenced the stimulation threshold. Sealed ends reduced the threshold compared to voltage-clamped conditions by a factor of approximately 5 to 100. Voltage-clamped axons are generally more difficult to excite, making sealed terminals more conservative for challenging the limits. However, cortical stimulation thresholds under clamped terminal conditions at 1 kHz are closer to the 50 V/m threshold (the lower tolerance interval of the active motor threshold) observed in transcranial magnetic stimulation than those under sealed terminals [12]. This suggests that voltage-clamped conditions better reflect a realistic scenario. It is important to note that we used a conservative assumption of large fiber thickness (20 μm diameter). For more common values of 1-5 μm [24], the thresholds are expected to increase by one to two orders of magnitude. Under these conditions, sealed ends may align more closely with experimentally observed thresholds, such as in a multi-scale modeling study of transcranial magnetic stimulation that used Blue Brain Project neural cells [24]. In this context, sealed thresholds would approach those of clamped conditions for a 20 μm fiber [27]. Thus, voltage-clamped conditions remain suitable for comparison with protection limits. In the case of ICNIRP, BRs apply a five-fold safety margin for occupational environments and a 10-fold reduction for the general public. In the case of IEEE, the DRLs apply safety factors of three for unrestricted environments and nine for restricted environments in the frequency range investigated in this study. Mean thresholds complied with the margins in all conditions. In the case of minimum thresholds, the margin was reduced at higher frequencies. The margins are satisfied with the minimum estimated cortical thresholds except at 100 kHz, where the limits of the restricted environment were near the minimum thresholds.

C. LIMITATIONS AND FUTURE WORK

First, an important consideration is that the excitation threshold strongly depends on how neuronal excitation is defined, especially at higher frequencies. The action potential is defined as depolarization over $V_T = 50$ mV and imposed conditions on action potential propagation over consecutive nodes of Ranvier. Varying depolarization threshold V_T or AP propagation conditions is expected to change the excitation thresholds. At higher frequencies, the typical action potential shape can be lost by fast membrane voltage oscillations occurring simultaneously at subsequent nodes. If these oscillation amplitudes are sufficient, they are considered action potentials under our conditions, potentially causing false positives. Proper identification of these could reduce non-compliant axons. Also, the gap between current exposure guidelines and obtained electro-stimulation thresholds is small in the high-frequency band, and sensitivity analysis of electrostimulation thresholds should also be considered. Second, as in the rationale for the safety guidelines/standard, we used neuronal excitation of an axon model constrained by boundary conditions to assess the conservativeness of safety guidelines. However, subthreshold electromagnetic fields below the action potential threshold are still capable of altering brain function [28]. Furthermore, morphologically

realistic models of human cortical cells, incorporating soma, dendritic trees, and axon collaterals, could enhance simulation accuracy. Future work should clarify subthreshold effects and the role of morphological realism in safety assessments. A source of uncertainty arises from electric conductivity variations (anisotropy, uniformity, and age dependency) [29], [30]. Third, this study highlights the importance of considering various head models because of the significant intersubject variability observed in three head models (Fig. 5). Future research should explore larger datasets and improved volume conductor models, such as diffusion tensor imaging and MRI-based anisotropic conductivities, for more accurate assessments of safety guideline conservativeness. Fourth, this study employed a uniform magnetic exposure scenario, which is consistent with conservative exposure assumptions used in international safety guidelines, which is considered the worst-case scenario. However, it is necessary to confirm whether uniform exposure can still be regarded as the worst-case scenario when using anatomical body models. In real-world settings, magnetic fields are often spatially nonuniform, leading to local variations in the induced electric fields and potentially different neural activation patterns and thresholds. Such exposure scenarios should also be considered to evaluate conservativeness. While such cases are beyond the scope of this study, our methodology could be extended to assess those configurations in future work. Finally, while electrophysiological data for direct validation of the numerical simulations remain limited, generating such data represents an important next step in refining this modeling approach.

V. CONCLUSION

We determined that the electric field limits established in both guidelines are conservative with the internal electric field needed for CNS stimulation in the intermediate frequency range, although the margin of conservativeness is reduced at higher frequencies when considering the strictest evaluations. For example, for voltage clamp conditions we observed 22.5-fold and 2.3-fold gaps between the lowest threshold and the unrestricted environment ICES guidelines at low-end (300 Hz – 1 kHz) and high-end (10 kHz - 100 kHz) frequencies, respectively. An extensive comparison considering more than 1.2 million scenarios from different nerve models, implementations, and head models provides a rationale for basing protection against adverse effects on PNS electrostimulation at intermediate frequencies. Future studies should revise the effects of higher frequencies that may affect the definition of stimulation thresholds that tend to be more compromised under the current results. Importantly, the results and methodology of this study could potentially contribute to the rationale and serve as input for the re-evaluation or updates of the intermediate frequency exposure guidelines.

ACKNOWLEDGMENT

The authors would like to IEEE/ICES/TC95/SC6 members for the valuable discussions during the conduction of this work. Grammar and language were reviewed using AI-assisted tools (ChatGPT (OpenAI) and Grammarly Inc.).

REFERENCES

[1] ICNIRP, "Guidelines for limiting exposure to time-varying electric and magnetic fields (1 Hz to 100 kHz)," *Health Phys.*, vol. 99, no. 6, pp. 818–836, Dec. 2010, doi: 10.1097/hp.0b013e3181f06c86.

[2] *IEEE Standard for Safety Levels With Respect to Human Exposure to Electric, Magnetic, and Electromagnetic Fields, 0 Hz to 300 GHz*, IEEE Standard C95.1-2019, 2019.

[3] J. P. Reilly, H. Antoni, M. A. Chilbert, and J. D. Sweeney, "Applied bioelectricity: From electrical stimulation to electropathology," *Appl. Bioelectricity, Electr. Stimulation Electropathology*, vol. 1, pp. 1–563, Aug. 1998.

[4] W. J. Havel, J. A. Nyenhuis, J. D. Bourland, K. S. Foster, L. A. Geddes, G. P. Graber, M. S. Waninger, and D. J. Schaefer, "Comparison of rectangular and damped sinusoidal dB/dt waveforms in magnetic stimulation," *IEEE Trans. Magn.*, vol. 33, no. 5, pp. 4269–4271, May 1997, doi: 10.1109/20.619732.

[5] T. Tarnaud, W. Joseph, L. Martens, and E. Tanghe, "Dependence of excitability indices on membrane channel dynamics, myelin impedance, electrode location and stimulus waveforms in myelinated and unmyelinated fibre models," *Med. Biol. Eng. Comput.*, vol. 56, no. 9, pp. 1595–1613, Sep. 2018, doi: 10.1007/s11517-018-1799-y.

[6] L. Firmin, P. Field, M. A. Maier, A. Kraskov, P. A. Kirkwood, K. Nakajima, R. N. Lemon, and M. Glickstein, "Axon diameters and conduction velocities in the macaque pyramidal tract," *J. Neurophysiol.*, vol. 112, no. 6, pp. 1229–1240, Sep. 2014.

[7] A. Opitz, M. Windhoff, R. M. Heidemann, R. Turner, and A. Thielscher, "How the brain tissue shapes the electric field induced by transcranial magnetic stimulation," *NeuroImage*, vol. 58, no. 3, pp. 849–859, Oct. 2011. [Online]. Available: http://www.ncbi.nlm.nih.gov/pubmed/21749927

[8] E. Neufeld, I. Vogiatzis Oikonomidis, M. Ida Iacono, L. M. Angelone, W. Kainz, and N. Kuster, "Investigation of assumptions underlying current safety guidelines on EM-induced nerve stimulation," *Phys. Med. Biol.*, vol. 61, no. 12, pp. 4466–4478, Jun. 2016, doi: 10.1088/0031-9155/61/12/4466.

[9] J. Gomez-Tames, I. Laakso, and A. Hirata, "Review on biophysical modelling and simulation studies for transcranial magnetic stimulation," *Phys. Med. Biol.*, vol. 65, no. 24, Dec. 2020, Art. no. 24TR03, doi: 10.1088/1361-6560/aba40d.

[10] J. P. Reilly and A. Hirata, "Low-frequency electrical dosimetry: Research agenda of the IEEE international committee on electromagnetic safety," *Phys. Med. Biol.*, vol. 61, no. 12, pp. R138–R149, Jun. 2016, doi: 10.1088/0031-9155/61/12/r138.

[11] I. Lagroye, "Gaps in knowledge relevant to the 'guidelines for limiting exposure to time-varying electric and magnetic fields (1 Hz–100 kHz)," *Health Phys.*, vol. 118, no. 5, pp. 533–542, 2020.

[12] M. Soldati, M. Mikkonen, I. Laakso, T. Murakami, Y. Ugawa, and A. Hirata, "A multi-scale computational approach based on TMS experiments for the assessment of electro-stimulation thresholds of the brain at intermediate frequencies," *Phys. Med. Biol.*, vol. 63, no. 22, Nov. 2018, Art. no. 225006, doi: 10.1088/1361-6560/aae932.

[13] Y. Suzuki, J. Gomez-Tames, Y. Diao, and A. Hirata, "Evaluation of peripheral electrostimulation thresholds in human model for uniform magnetic field exposure," *Int. J. Environ. Res. Public Health*, vol. 19, no. 1, p. 390, Dec. 2021, doi: 10.3390/ijerph19010390.

[14] P. P. M. So, M. A. Stuchly, and J. A. Nyenhuis, "Peripheral nerve stimulation by gradient switching fields in magnetic resonance imaging," *IEEE Trans. Biomed. Eng.*, vol. 51, no. 11, pp. 1907–1914, Nov. 2004, doi: 10.1109/TBME.2004.834251.

[15] J. Gomez-Tames, T. Tarnaud, K. Miwa, A. Hirata, T. Van de Steene, L. Martens, E. Tanghe, and W. Joseph, "Brain cortical stimulation thresholds to different magnetic field sources exposures at intermediate frequencies," *IEEE Trans. Electromagn. Compat.*, vol. 61, no. 6, pp. 1944–1952, Dec. 2019, doi: 10.1109/TEMC.2019.2943138.

[16] I. Laakso, S. Tanaka, S. Koyama, V. De Santis, and A. Hirata, "Intersubject variability in electric fields of motor cortical tDCS," *Brain Stimulation*, vol. 8, no. 5, pp. 906–913, Sep. 2015, doi: 10.1016/j.brs.2015.05.002.

[17] T. W. Dawson and M. A. Stuchly, "Analytic validation of a three-dimensional scalar-potential finite-difference code for low-frequency magnetic induction," *Appl. Comput. Electromagn. Soc. J.*, vol. 11, pp. 72–81, Nov. 1996.
[18] I. Laakso and A. Hirata, "Fast multigrid-based computation of the induced electric field for transcranial magnetic stimulation," *Phys. Med. Biol.*, vol. 57, no. 23, pp. 7753–7765, Dec. 2012, doi: 10.1088/0031-9155/57/23/7753.
[19] S. Gabriel, R. W. Lau, and C. Gabriel, "The dielectric properties of biological tissues: III. Parametric models for the dielectric spectrum of tissues," *Phys. Med. Biol.*, vol. 41, no. 11, pp. 2271–2293, Nov. 1996, doi: 10.1088/0031-9155/41/11/003.
[20] D. R. McNeal, "Analysis of a model for excitation of myelinated nerve," *IEEE Trans. Biomed. Eng.*, vol. BME-23, no. 4, pp. 329–337, Jul. 1976.
[21] L. A. Cartee, "Evaluation of a model of the cochlear neural membrane. II: Comparison of model and physiological measures of membrane properties measured in response to intrameatal electrical stimulation," *Hearing Res.*, vol. 146, nos. 1–2, pp. 153–166, Aug. 2000, doi: 10.1016/s0378-5955(00)00110-6.
[22] X. Zhang, J. R. Roppolo, W. C. de Groat, and C. Tai, "Mechanism of nerve conduction block induced by high-frequency biphasic electrical currents," *IEEE Trans. Biomed. Eng.*, vol. 53, no. 12, pp. 2445–2454, Dec. 2006. [Online]. Available: http://ieeexplore.ieee.org/xpls/abs_all.jsp?arnumber=4015624
[23] R. Fitzhugh, "Computation of impulse initiation and saltatory conduction in a myelinated nerve fiber," *Biophys. J.*, vol. 2, no. 1, pp. 11–21, Jan. 1962, doi: 10.1016/s0006-3495(62)86837-4.
[24] A. S. Aberra, A. V. Peterchev, and W. M. Grill, "Biophysically realistic neuron models for simulation of cortical stimulation," *J. Neural Eng.*, vol. 15, no. 6, Dec. 2018, Art. no. 066023, doi: 10.1088/1741-2552/aadbb1.
[25] J. Gomez–Tames, I. Laakso, T. Murakami, Y. Ugawa, and A. Hirata, "TMS activation site estimation using multiscale realistic head models," *J. Neural Eng.*, vol. 17, no. 3, Jun. 2020, Art. no. 036004, doi: 10.1088/1741-2552/ab8ccf.
[26] I. Laakso and A. Hirata, "Reducing the staircasing error in computational dosimetry of low-frequency electromagnetic fields," *Phys. Med. Biol.*, vol. 57, no. 4, pp. N25–N34, Feb. 2012, doi: 10.1088/0031-9155/57/4/n25.
[27] J. P. Reilly, "Peripheral nerve stimulation by induced electric currents: Exposure to time-varying magnetic fields," *Med. Biol. Eng. Comput.*, vol. 27, no. 2, pp. 101–110, Mar. 1989, doi: 10.1007/bf02446217.
[28] C. J. Stagg, A. Antal, and M. A. Nitsche, "Physiology of transcranial direct current stimulation," *J. ECT*, vol. 34, no. 3, pp. 144–152, Sep. 2018, doi: 10.1097/yct.0000000000000510.
[29] M. De Lucia, G. J. M. Parker, K. Embleton, J. M. Newton, and V. Walsh, "Diffusion tensor MRI-based estimation of the influence of brain tissue anisotropy on the effects of transcranial magnetic stimulation," *NeuroImage*, vol. 36, no. 4, pp. 1159–1170, Jul. 2007, doi: 10.1016/j.neuroimage.2007.03.062.
[30] B. Howell and C. C. McIntyre, "Analyzing the tradeoff between electrical complexity and accuracy in patient-specific computational models of deep brain stimulation," *J. Neural Eng.*, vol. 13, no. 3, Jun. 2016, Art. no. 036023, doi: 10.1088/1741-2560/13/3/036023.

JOSE GOMEZ-TAMES (Member, IEEE) received the B.S. degree in electronics engineering from Costa Rica Institute of Technology, Costa Rica, in 2007, and the M.S. and Ph.D. degrees in medical system engineering from Chiba University, Chiba, Japan, in 2012 and 2015, respectively. From 2007 to 2009, he was an Instructor with the Institute of Technology of Costa Rica. From 2015 to 2016, he was a Research Fellow with Japan Society for the Promotion of Science. He joined Nagoya Institute of Technology, in 2016, as a Research Assistant Professor, later advancing to a Research Associate Professor and then an Associate Professor, in 2020. Since 2022, he has been an Associate Professor with the Department of Medical Systems Engineering, School of Engineering, Chiba University, Japan. His research interests include computational bioelectromagnetics, neural engineering, and neuromodulation.

THOMAS TARNAUD was born in Wilrijk, Belgium, in May 1993. He received the M.Sc. degree in engineering physics from Ghent University, Belgium, in July 2016, and the Ph.D. degree, in March 2021. From August 2016 to December 2020, he was a Ph.D. Fellow with the Research Foundation Flanders (FWO-V), Department of Information Technology (INTEC), Ghent University. Since March 2021, he has been a Postdoctoral Researcher at INTEC, WAVES, Ghent University, and in October 2021, he was a Postdoctoral Fellow with FWO. From August to November 2022, he stayed at the Translational Neural Engineering Laboratory of École Polytechnique Fédérale de Lausanne, Switzerland, to conduct research on automated and experimentally validated computational pipelines for ultrasound neuromodulation of peripheral nerves. From May to June 2023, he performed research at the Electromagnetics in Health Technology Laboratory of Aalto University, Finland, on realistic axon models derived from diffusion tractography for transcranial magnetic stimulation. Since October 2024, he has been an Associate Professor at WAVES (INTEC) and 4Brain (Department of Neurology) Research Groups. From January 2025 to December 2029, he was the PI of an ERC-funded project to develop a closed-loop ultrasound neuromodulation treatment for epilepsy. His research is focused on computational modeling of electrical and ultrasonic neuromodulation, electromagnetic safety and neural engineering. His research focused on computational modeling of electrical and ultrasonic neuromodulation, electromagnetic safety, and neural engineering.

WOUT JOSEPH (Senior Member, IEEE) received the Ph.D. degree, in 2005. From 2007 to 2013, he was a Postdoctoral Fellow with Research Foundation Flanders. Since October 2009, he has been a Professor of experimental characterization of wireless communication systems with Ghent University, Ghent, Belgium. His research interests include electromagnetic field exposure assessment, propagation, and wireless performance analysis for wireless communication systems, antennas, calibration, and green networks.

EMMERIC TANGHE was born in Tielt, Belgium, in August 1982. He received the M.Sc. and Ph.D. degrees in electrical engineering from Ghent University, Ghent, Belgium, in 2005 and 2011, respectively. From September 2005 to May 2011, he was a Research Assistant with the Department of Information Technology, IMEC, Ghent University (UGent/INTEC). His scientific work focused on the modeling of indoor and outdoor propagation through field measurements. Since May 2011, he has been a Postdoctoral Researcher with Ghent University and continues his work in propagation modeling. From October 2012 to September 2018, he was a Postdoctoral Fellow of the Research Foundation-Flanders (FWO-V). In October 2015, he became a part-time Professor of medical applications of electromagnetic fields in and around the human body.